Subramanyan Vasudevan[1]
Florence Epron[2]
Jothinathan Lakshmi[1]
Subbiah Ravichandran[1]
Swaminathan Mohan[1]
Ganapathy Sozhan[1]

[1]Central Electrochemical Research Institute (CSIR), Karaikudi, India.

[2]Laboratoire de Catalyse en Chimie Organique, Universite de Poitiers, CNRS, Poitiers, France.

Short Communication

Removal of NO_3^- from Drinking Water by Electrocoagulation – An Alternate Approach

The present study provides an electrocoagulation method, for the removal of NO_3^- from drinking water using magnesium as the anode and cathode. The experiments are carried out as a function of pH, temperature, and current density. The results show that the maximum removal efficiency of 95.8% was achieved at a current density of 0.25 A/dm^2, at a pH of 7.0. The adsorption of NO_3^- preferably fitting the Langmuir adsorption isotherm suggests monolayer coverage of the adsorbed molecules. The adsorption process follows a second-order kinetics model. Thermodynamic studies show that the adsorption was exothermic and spontaneous in nature.

Keywords: Adsorption kinetics; Clean technology; Electrocoagulation; Isotherms; NO_3^- removal

Received: October 23, 2009; *revised:* November 30, 2009; *accepted:* December 9, 2009

DOI: 10.1002/clen.200900226

1 Introduction

As is well known, methemoglobinemia (blue-baby syndrome) is one of the main human health problems caused by high levels of nitrate in drinking water. Other potential health effects associated with high levels of nitrates are cancer and tumors [1 – 3]. The World Health Organization (WHO) has set the drinking water guideline values for nitrate, nitrite, and ammonia at 50 mg/L, 0.5 mg/L, and 0.5 mg/L, respectively [4]. Thus, their removal gains more and more attention. Current methods for the removal of NO_3^- from ground water are limited to physiochemical and biological methods [5 – 8]. The physiochemical processes include ion exchange, reduction, and membrane separation methods. The removal of NO_3^- by ion exchange methods is feasible from an economic standpoint, but it is nonspecific for the ions of interest and yields copious amounts of concentrated brines containing sulfate, chloride, and NO_3^-, each of which must be disposed off separately. Recently, metallic iron and aluminium powder were used to reduce NO_3^- in water; however, this reduction process is highly dependent on the pH. Membrane separation techniques yield concentrated brines and are cost-prohibitive on a large scale. Biological denitrification can selectively remove NO_3^- with little waste. However, this process is complex and requires careful monitoring of the carbon source. Most current NO_3^- removal processes have various limitations and, in particular, are not suitable for small communities. Recent research has demonstrated that electrochemical reduction offers an attractive alternative to the above-mentioned traditional methods for treating nitrate contaminated water [9 – 16]. Nonetheless, the process is limited in practice due to the formation of by-products like nitrite and ammonia during treatment [17 – 19]. The nitrite and ammonia by-products are subsequently oxidized to nitrate and nitrogen, respectively, by oxidants, either generated by in-situ or ex-situ methods, before further use [20]. The challenge is to find a suitable process to avoid/limit the formation of nitrite and ammonia in treated water. The aim of this work was to investigate the adsorption of NO_3^- by a coagulant, generated in-situ, by the anodic dissolution of magnesium and to find effective conditions that avoid/limit the formation of nitrite and ammonia in the electrocoagulation process. In this process, anodic dissolution of the metal electrode takes place with the evolution of hydrogen gas at the cathode. Electrochemically generated metal ions from these electrodes can undergo hydrolysis near the anode to produce a series of activated intermediates that are able to destabilize the finely dispersed particles present in the water to be treated. The destabilized particles then aggregate to form flocks as outlined below. When magnesium is used as the electrode, the reactions are as follows, Eqs. (1) – (3):

$$\text{At the cathode: } 2\,H_2O + 2\,e^- \rightarrow H_2\,(g) + 2\,OH^- \quad (1)$$

$$\text{At the anode: } Mg \rightarrow Mg^{2+} + 2\,e^- \quad (2)$$

$$\text{In the solution: } Mg^{2+}\,(aq) + 2\,H_2O \rightarrow Mg(OH)_2\downarrow + 2\,H^+\,(aq) \quad (3)$$

2 Material and Methods

2.1 Cell Construction and Electrolysis

The electrolytic cell [21] consisted of a 1.0 L Plexiglas vessel that was fitted with a polycarbonate cell cover with slots to introduce the anode, cathode, pH sensor, thermometer, and electrolytes. Magnesium sheets (Alfa Aesar), of surface area (0.02 m^2), acted as the anode and cathode, with an interelectrode distance of 0.005 m. The temperature of the electrolyte was controlled to the desired value, with a variation of ± 2 K, by adjusting the rate of flow of thermostatically controlled water through an external glass-cooling spiral. A regulated direct current (DC) was supplied from a rectifier (10 A, 0 – 25 V, Aplab model). The nitrate (KNO_3) (Analar Reagent) was dissolved in distilled water at the required concentration (300 – 700 mg/L). 0.90 L of solution was used as the electrolyte for each experiment. The pH

Correspondence: Dr. S. Vasudevan, Central Electrochemical Research Institute (CSIR), Karaikudi – 630 006, India.
E-mail: vasudevan65@gmail.com

Table 1. Final concentrations of nitrate, nitrite and ammonia at different current densities at pH 7

Current Density, (A/dm^2)	Final Concentration, (mg/L)		
	Nitrate	Nitrite	Ammonia
0.10	35.0	0.05	0.06
0.15	29.2	0.07	0.08
0.25	21.3	0.10	0.09
0.50	19.7	0.12	0.10
0.75	18.4	0.15	0.11

of the electrolyte was adjusted, if required, with 1 M HCl or 1 M NaOH solutions before the adsorption experiments.

2.2 Analysis

All analysis was carried out according to standard methods [22]. Nitrate was determined using a UV-VIS spectrophotometer (MERCK-Pharo 300, Germany) and nitrite was analyzed by ion chromatography (Metrohm AG, Switzerland). The determination of ammonia was performed using an ion meter (TOA-DKK, Japan). XRD was used to analyze the magnesium hydroxide (XRD, JEOL, Japan).

3 Results and Discussion

3.1 Effects of Current Density and pH

Current density is one of the imperative operational parameters in elecrocoagulation processes. A series of experiments were carried out to investigate the effects of current density, using 500 mg/L nitrate containing solutions, at pH 7.0, with current density being varied from 0.1 – 0.75 A/dm^2. The NO_3^- removal efficiencies were 93.0, 94.2, 95.8, 95.9, and 96.2% for current densities 0.1, 0.15, 0.25, 0.5, and 0.75 A/dm^2, respectively. From the results, it was found that at current densities higher than 0.25 A/dm^2 the removal efficiency remained almost constant. This expected behavior is easily explained by the increase in the coagulation rate when the current is increased, which indicates that the adsorption depends upon the availability of nitrate binding sites [23]. When the current density is increased, the energy consumption also increases rapidly. The results listed in Tab. 1 show the final concentrations of nitrate, nitrite, and ammonia at different current densities. These values are in agreement with the WHO drinking water standards.

It has been established that the initial pH of the electrolyte is one of the important factors affecting the performance of the electrochemical process, particularly the performance of the electrocoagulation process [24]. To evaluate its effect, a series of experiments were performed, using 500 mg/L nitrate-containing solutions with an initial pH varying in the range from 3 – 10. The maximum removal efficiency of 95.8% was obtained at pH 7. The minimum nitrate removal efficiency was 84.5% at pH 10. At alkaline pH, the oxide surface has a net negative charge and would tend to repulse the anionic nitrate in solution. Therefore, the maximum amount of nitrate removal occurred at pH 7.

3.2 Effect of Initial Nitrate Concentration

The adsorption capacity of nitrate was examined at different nitrate concentrations (300 – 700 mg/L). The amount of nitrate adsorbed

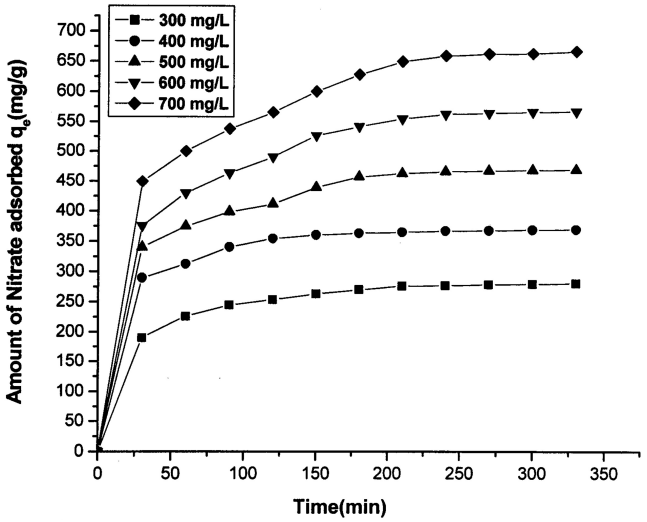

Figure 1. Effect of agitation time and initial nitrate concentration on the amount of nitrate adsorbed (q_e vs. t). Conditions are electrolyte pH: 7; electrolyte temperature: 303 K, and current density: 0.25 A/dm^2.

increased with increasing nitrate concentration and remained nearly constant after reaching equilibrium. The results in Fig. 1 show the plot of q_e vs. t. From the data in Fig. 1, it was found that, for all the concentrations studied, the equilibrium time was reached after 60 min. The amount of nitrate adsorbed, q_e, increased from 282 – 669.2 mg/g as the concentration was increased from 300 – 700 mg/L. The adsorption was rapid in the initial stages and gradually decreased as the adsorption progressed. The plots are single, smooth, and continuous curves leading to saturation, suggesting possible monolayer coverage of nitrate on the surface of the adsorbent [25].

3.3 Adsorption Kinetics

First-order [26] and second-order [27] kinetics were applied to the experimental data, in order to investigate the adsorption kinetics of nitrate onto magnesium hydroxide. The linear form of Lagergren's first-order rate equation is as follows, Eq. (4)

$$\log(q_e - q_t) = \log(q_e) - k_1\, t/2.303 \tag{4}$$

A linear fit of $\log(q_e - q_t)$ vs. t shows the applicability of this kinetic model. The first-order rate constant, k_1, and q_e values were determined from the slope and intercept, respectively. The integrated linear form of the second-order equation is given by Eq. (5):

$$t/q_e = 1/k_2\, q_e^2 + t/q_e \tag{5}$$

where k_2 is the second-order rate constant determined from a plot of t/q_t vs. time, Fig. 2. Straight line plots were obtained for the first-order and second-order reaction of nitrate adsorption. The calculated values of k_1, k_2, q_e, and their corresponding regression coefficient values, R^2, are presented in Tab. 2. It was found that the calculated q_e values did not agree with the experimental q_e values, with low regression values for the first-order case, suggesting that this adsorption system was not first-order. The calculated q_e values agreed very well with the experimental values for second-order

Table 2. Comparison between the experimental and calculated q_e values for different initial nitrate concentrations in the first- and second-order adsorption isotherms at temperature 305 K and pH 7.

Concentration, (mg/L)	q_e, (exp)	First-order Adsorption			Second-order Adsorption		
		q_e (Cal)	$K_1 \cdot 10^4$ (min/mg)	R^2	q_e (Cal)	$K_2 \cdot 10^4$ (min/mg)	R^2
300	226.2	25.36	0.326	0.7563	225.3	0.3264	0.9996
400	313.0	34.94	0.336	0.6654	312.2	0.3229	0.9956
500	375.1	45.43	0.456	0.5362	374.2	0.4362	0.9941
600	430.2	52.21	0.465	0.7789	432.2	0.4460	0.9995
700	501.6	60.76	0.499	0.6989	500.2	0.5522	0.9952

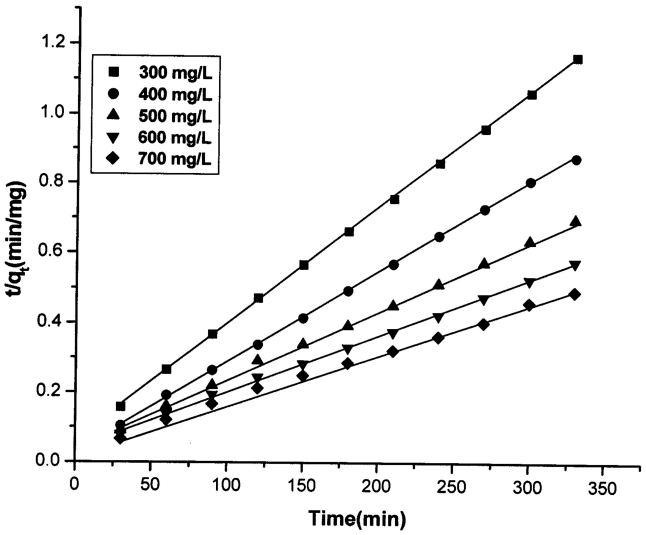

Figure.2. Second-order kinetic model plot (t/q_t vs. t) of different concentrations of nitrate. Conditions are electrolyte pH: 7; electrolyte temperature: 303 K, and current density: 0.25 A/dm^2.

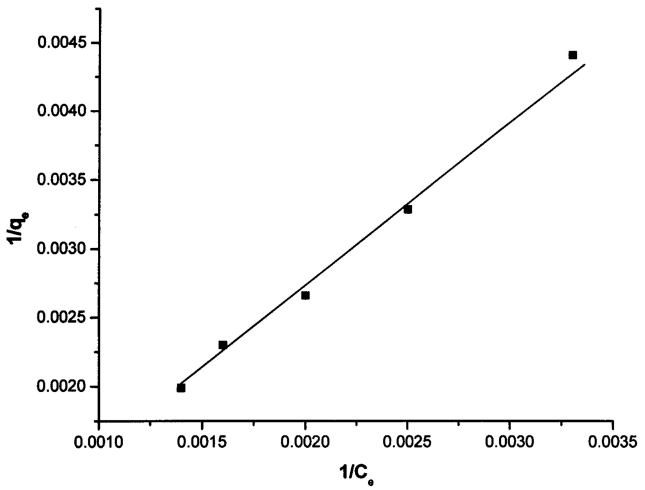

Figure.3. Langmuir plot ($1/q_e$ vs. $1/C_e$). Conditions are electrolyte pH: 7; electrolyte temperature: 303 K, and current density: 0.25 A/dm^2.

kinetics and a regression coefficient of above 0.99 showed that the adsorption system is second-order.

3.4 Adsorption Isotherms

The adsorption isotherms were analyzed using Langmuir [28] and Freundlich [29] isotherm models. The logarithmic form of the Freundlich isotherm is given in Eq. (6):

$$\log q_e = \log k_f + n \log C_e \quad (6)$$

where k_f is the Freundlich constant related to adsorption capacity, n is the energy or intensity of adsorption, and C_e is the equilibrium concentration of nitrate (mg/L). k_f and n can be obtained from the slope and intercept of the plot of $\log q_e$ against $\log C_e$. An n value falling in the range from 1 – 10 indicates favorable sorption. The Freundlich isotherms k_f and n values are 8.248 (mg/g) and 6.361 (L/mg), respectively, with a regression value, R^2, of 0.9945. The linearized form of the Langmuir adsorption isotherm model is given by Eq. (7):

$$C_e/q_e = 1/q_m K_a + C_e/q_m \quad (7)$$

where C_e is the concentration of the nitrate solution (mg/L) at equilibrium, q_m is the adsorption capacity (Langmuir constant), and k_a is the energy of adsorption. The q_m and k_a values are 5801.94 mg/g and 0.795 L/g, respectively, with an R^2 value of 0.9976, obtained from the slope and intercept of $1/C_e$ vs. $1/q_e$, Fig. 3. The higher regression value of the Langmuir isotherm compared to that of the Freundlich isotherm shows that the adsorption of NO_3^- follows the Langmuir isotherm.

3.5 Thermodynamic Studies

The thermodynamic parameters are considered to be the actual indicators for the application of a process. The free energy change, ΔG^0, enthalpy change, ΔH^0, and entropy change, ΔS^0, were calculated from the variation of the thermodynamic equilibrium constant, K, with temperature. The free energy change was obtained using the following relationship, Eq. (8):

$$\Delta G^0 = -\mathrm{R}\,T \ln K_c \quad (8)$$

where ΔG^0 is the change in free energy (kJ/mol), K_c is the equilibrium constant, R is the gas constant, and T is the temperature in K. Other thermodynamic parameters, such as entropy change, ΔS^0, and enthalpy change, ΔH^0, were determined using the van't Hoff equation, Eq. (9):

$$\log K_c = \frac{\Delta S^0}{2.303\mathrm{R}} - \frac{\Delta H^0}{2.303\mathrm{R}T} \quad (9)$$

Table 3. Comparison between the experimental and calculated q_e values for different initial nitrate concentrations of 500 mg/L in the first- and second-order adsorption isotherms at various temperatures and pH 7.

Temperature, (K)	q_e, (exp)	First-order Adsorption			Second-order Adsorption		
		q_e (Cal)	$K_1 \cdot 10^4$ (min/mg)	R^2	q_e (Cal)	$K_1 \cdot 10^4$ (min/mg)	R^2
313	390.2	36.21	0.326	0.6652	385.7	0.4163	0.9983
323	403.6	42.23	0.336	0.6736	391.5	0.4199	0.9851
333	410.7	53.61	0.396	0.5930	400.3	0.4206	0.9879
343	417.3	61.23	0.401	0.6021	409.2	0.4391	0.9944

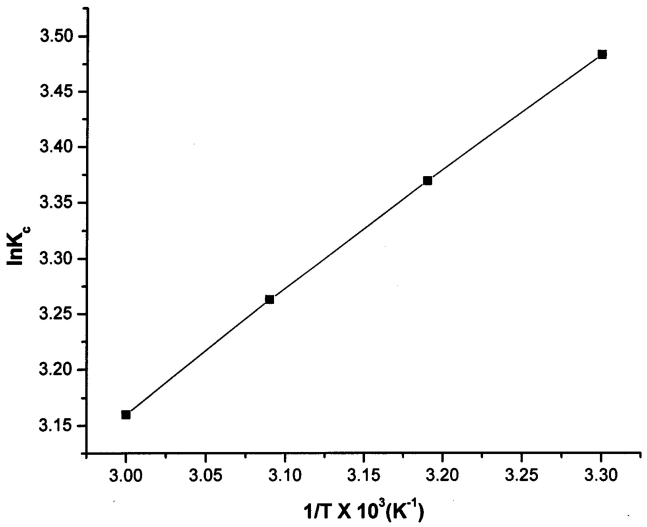

Figure 4. Plot of $\ln K_c$ vs $1/T$. Conditions are electrolyte pH: 7 and current density: 0.25 A/dm^2.

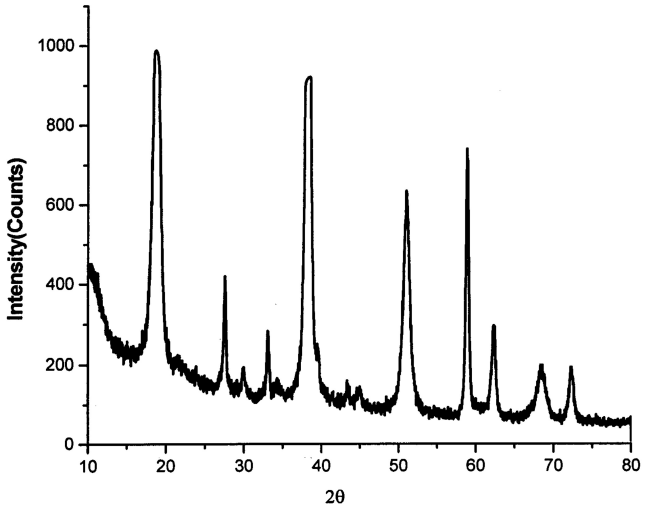

Figure.5. XRD diffractogram showing the electrocoagulation by-product of the magnesium anode.

The enthalpy change, ΔH^0, and entropy change, ΔS^0, were obtained from the slope and intercept of the van't Hoff from linear plots of $\ln K_c$ vs. $1/T$, Fig. 4. The values of the free energy change for adsorption, ΔG^0, are −15.031, −13.029, −12.031, and −10.025 kJ/mol at temperatures of 303, 313, 323, and 333 K, respectively. The enthalpy of adsorption, ΔH^0, is −12.90 kJ/mol and the entropy of adsorption, ΔS^0, is 26.33 J/K mol. A negative value of enthalpy change, ΔH^0, indicates that the adsorption process is exothermic in nature and the negative value of change in free energy, ΔG^0, shows the spontaneous adsorption of nitrate on the adsorbent. Positive values of entropy change show the increased randomness of the solution interface during the adsorption of nitrate on the adsorbent [30]. First-order rate constants and correlation coefficients were calculated for different temperatures using the Lagergren rate equation, i.e., 303 – 333 K. The calculated 'q_e' values obtained from the first-order kinetics do not agree with the experimental 'q_e' values. The second-order kinetics model shows that the calculated 'q_e' values agree with the experimental values, Tab. 3. This indicates that the adsorption follows the second-order kinetic model at the different temperatures used in this study. From the table, it was found that the rate constant, k_2, increased on increasing the temperature from 305 – 333 K. The increase in adsorption may be due to a change in pore size on increasing the kinetic energy of the nitrate species, resulting in an enhanced rate of intraparticle adsorbate diffusion.

3.6 XRD and FTIR Analysis

The X-ray diffraction pattern of the magnesium electrode coagulant showed well defined crystalline phases, such as magnesium nitrate at 26.667° and magnesium hydroxide at 38.016°, Fig. 5. The FT-IR spectrum of the nitrate-magnesium hydroxide shows a sharp and strong peak at 3698.07 cm^{-1} due to the O – H stretching vibration in the $Mg(OH)_2$ structures. The peak at 1639.72 cm^{-1} indicates the bending vibration of H – O – H. A broad absorption band at 3448.60 cm^{-1} is suggestive of the transformation from free protons into a proton-conductive state in brucite. A strong absorbance band at 1383.89 cm^{-1} represents the Mg-nitrate linkage [31] and a strong peak at 475.51 cm^{-1} is assigned to the Mg – O stretching vibration.

4 Conclusions

The results showed that the optimized removal efficiency of 95.8% was achieved at an optimum current density of 0.25 A/dm^2 and a pH of 7.0 using magnesium as the anode and cathode with an energy consumption of 2.34 kWh/m^3. The magnesium hydroxide generated in the cell adsorbs both nitrate and nitrite, present in the water, and reduced the concentration to less than 45 mg/L and 0.5 mg/L, respectively. Furthermore, there was no ammonia contaminant in the treated water. The results also indicate that electrocoagulation

is an attractive alternative process for the removal of nitrate from drinking water. The adsorption of nitrate fits the Langmuir adsorption isotherm preferably, suggesting monolayer coverage of the adsorbed molecules. The adsorption process follows second-order kinetics. Temperature studies showed that adsorption was exothermic and spontaneous in nature.

Acknowledgements

The authors thank the Indo-French Centre for the Promotion of Advanced Research (IFCPAR), New Delhi, India for financial support for this project (3800-W1). The authors wish to express their gratitude to the Director, Central Electrochemical Research Institute, Karaikudi, for assistance with publishing this article.

The authors have declared no conflict of interest.

References

[1] P. J. Squillace et al., VOC's, Pesticides, Nitrate, and Their Mixtures in Groundwater Used for Drinking Water in the United States, *Environ. Sci. Technol.* **2002**, *36*, 1922.

[2] S. K. Gupta et al., Recurrent Acute Respiratory Tract Infections in Areas with High Nitrate Concentrations in Drinking Water, *Environ. Health Perspect.* **2000**, *108*, 363.

[3] H. Yang, H. Cheng, Controlling Nitrite Level in Drinking Water by Chlorination and Chloramination, *Sep. Purif. Technol.* **2007**, *56*, 392.

[4] *WHO Guidelines for Drinking Water Quality: Health Criteria and Other Supporting Information*, 3rd ed., WHO, Geneva **2004**.

[5] V. Mateju, S. Cizinska, J. Krejci, J. Tomas, Biological Water Denitrification – A Review, *Enzyme Microb. Technol.* **1992**, *14*, 170.

[6] P. A. Terry, Removal of Nitrates and Phosphates by Ion Exchange with Hydrotalcite, *Environ. Eng. Sci.* **2009**, *26*, 691.

[7] U. S. Orlando, A. U. Baes, W. Nishijima, M. Okada, Preparation of Agricultural Residue Anion Exchangers and Its Nitrate Maximum Adsorption Capacity, *Chemosphere* **2002**, *48*, 1041.

[8] O. Primo, M. J. Rivero, A. M. Urtiaga, I. Ortiz, Nitrate Removal from Electrooxidized Landfill Leachate by Ion Exchange, *J. Hazard. Mater.* **2009**, *164*, 389.

[9] O. A. Petri, T. Y. Safonova, Electroreduction of Nitrate and Nitrite Anions on Platinum Metals: A Model Process for Elucidating the Nature of the Passivation by Hydrogen Adsorption, *J. Electroanal. Chem.* **1992**, *331*, 897.

[10] L. J. J. Janssen, M. M. J. Pieterse, E. Barendrecht, Reduction of Nitric Oxide at a Platinum Cathode in an Acidic Solution, *Electrochim. Acta* **1977**, *22*, 27.

[11] A. C. A. de Vooys, R. A. van Santen, J. A. R. van Veen, Electrocatalytic Reduction of NO_3^- on Palladium/Copper Electrodes, *J. Mol. Catal. A: Chem.* **2000**, *154*, 203.

[12] M. Li, C. Feng, Z. Zhang, N. Sugiura, Efficient Electrochemical Reduction of Nitrate to Nitrogen Using Ti/IrO_2-Pt Anode and Different Cathodes, *Electrochim. Acta* **2009**, *54*, 4600.

[13] I. Katsounaros, D. Ipsakis, C. Polatides, G. Kyriacou, Efficient Electrochemical Reduction of Nitrate to Nitrogen on Tin Cathode at Very High Cathodic Potentials, *Electrochim. Acta* **2006**, *52*, 1329.

[14] B. P. Dash, S. Chaudhari, Electrochemical Denitrification of Simulated Groundwater, *Water Res.* **2005**, *39*, 4065.

[15] Z. Mácová, K. Bouzek, Electrocatalytic Activity of Copper Alloys for Reduction in a Weakly Alkaline Solution Part 1: Copper – Zinc, *J. Appl. Electrochem.* **2005**, *35*, 1203.

[16] K. Tada, K. Shimazu, Kinetic Studies of Reduction of Nitrate Ions at Sn-modified Pt Electrodes Using a Quartz Crystal Microbalance, *J. Electroanal. Chem.* **2005**, *577*, 303.

[17] C. Polatides, M. Dortsiou, G. Kyriacou, Electrochemical Removal of Nitrate Ion from Aqueous Solution by Pulsing Potential Electrolysis, *Electrochim. Acta* **2005**, *50*, 5237.

[18] L. M. Devkota et al., Variation of Oxidation–Reduction Potential Along the Breakpoint Curves in Low Ammonia Effluents, *Water Environ. Res.* **2000**, *72*, 610.

[19] J.-K. Lee et al., Residual Chlorine Distribution and Disinfiction during Electrochemical Removal of Dilute Ammonia from an Aqueous Solution, *J. Chem. Eng. Jpn.* **2002**, *35*, 285.

[20] M. Li et al., Simultaneous Reduction of Nitrate and Oxidation of Byproducts Using Electrochemical Methods, *J. Hazard. Mater.* **2009**, *171*, 724.

[21] S. Vasudevan, J. Lakshmi, J. Jayaraj, G. Sozhan, Remediation of Phosphate Contaminated Water by Electrocoagulation with Aluminum, Aluminum Alloy and Mild Steel Anodes, *J. Hazard. Mater.* **2009**, *164*, 1480.

[22] *Standard Methods for the Examination of Water and Wastewater*, Water Pollution Control Federation, American Public Health Association (APHA), Washington, DC **1998**.

[23] S. Vasudevan, J. Lakshmi, G. Sozhan, Studies on the Removal of Iron from Drinking Water by Electrocoagulation – A Clean Process, *Clean – Soil, Air, Water* **2009**, *37*, 45.

[24] S. Vasudevan et al., Studies on the Removal of Phosphate from Drinking Water by an Electrocoagulation Process, *Ind. Eng. Chem. Res.* **2008**, *47*, 2018.

[25] C. Namasivayam, K. Prathap, Recycling Fe(III)/Cr(III) Hydroxide, an Industrial Solid Waste for the Removal of Phosphate from Water, *J. Hazard. Mater.* **2005**, *123B*, 127.

[26] I. S. Lyubchik et al., Kinetics and Thermodynamics of the Cr(III) Adsorption on the Activated Carbon from Co-mingled Wastes, *Colloids Surf. A* **2004**, *242*, 151.

[27] C. Namasivayam, S. Senthil Kumar, Removal of Arsenic(V) from Aqueous Solutions Using Industrial Solid Waste: Adsorption Rates and Equilibrium Studies, *Ind. Eng. Chem. Res.* **1998**, *37*, 4816.

[28] F. H. Uber, Dye Adsorption in Lösungen, *Z. Phys. Chem.* **1985**, *57*, 387.

[29] I. Langmuir, The Adsorption of Gases on Plane Surface of Gases on Plane Surface of Glass, Mica and Platinum, *J. Am. Chem. Soc.* **1918**, *40*, 1361.

[30] S. Vasudevan, J. Jayaraj, J. Lakshmi, G. Sozhan, Removal of Iron from Drinking Water by Electrocoagulation: Adsorption and Kinetics Studies, *Korean J. Chem. Eng.* **2009**, *26*, 1058.

[31] Q.-Z. Yang et al., Studies on Synthesis and Properties of Mg-Al-Nitrate Layered Double Hydroxides, *Chin. Chem. Lett.* **2003**, *14*, 79.

